Synthesis and Molecular Structures of Novel α-Amino Organoaluminum Ester Enolates. Key Intermediates in the Selective Formation of *trans*-3-Amino-2-azetidinones

Fred H. van der Steen,† Guido P. M. van Mier,† Anthony L. Spek,‡ Jan Kroon,‡ and Gerard van Koten*,†

Contribution from the Debye Research Institute, Department of Metal-Mediated Synthesis, University of Utrecht, Padualaan 8, 3584 CH Utrecht, The Netherlands, and Bijvoet Research Institute, Laboratory for Crystal and Structural Chemistry, University of Utrecht, Padualaan 8, 3584 CH Utrecht, The Netherlands. *Received November 30, 1990*

Abstract: This paper describes the synthesis, characterization, and synthetic application of new α-amino dialkylaluminum ester enolates. With simple imines, these in situ prepared aluminum enolates afford *trans*-3-amino-2-azetidinones **5** and **6** with good de's (72–92%) in excellent yields when an (small) excess of dialkylaluminum chloride is present. Transmetalation of LiO(RO)C=C(H)NR^{1}R^2 (**2**, R = R^1 = R^2 = alkyl) with (R^3)$_2$AlCl (R^3 = alkyl) affords pure (R^3)$_2$AlO(RO)C=C(H)NR^{1}R^2 (**3**) in quantitative yields. Upon addition of a second equivalent of (R^3)$_2$AlCl, stable adducts (R^3)$_2$AlO[(RO)C=C(H)-NR^{1}R^2]→Al(R^3)$_2$Cl (**3'**) are formed. In both types of enolates, the ester enolate anions are N,O-chelate bound to the metal centers through Al–O and dative Al–N bonds. Consequently, the configuration of these enolates is *Z*. A crystal structure determination of **3b** (R = R^1 = R^2 = R^3 = Me) shows a dimeric associate, having a planar skeleton, consisting of two symmetry-related AlOCCN units (Al–O = 1.853 (3) Å, Al–N = 2.260 (3) Å), that are connected via Al–O–Al bridges (Al–O^{dative} = 2.055 (3) Å). The aluminum centers are five-coordinated with a slightly distorted trigonal bipyramidal geometry. Enolate **3b** crystallizes as colorless crystals in the space group $P2_1/n$ with a = 8.095 (1) Å, b = 13.747 (1) Å, c = 9.641 (2) Å, β = 104.41 (1)°, V = 1039.1 (3) Å^3, Z = 2, and T = 295 K. Full-matrix least-squares refinement on F converged at R = 0.056 and R_w = 0.057. A crystal structure determination of **3b'** (R = R^1 = R^2 = R^3 = Me) shows a dinuclear monomeric adduct, consisting of a planar AlOCCN unit (Al–O = 1.870 (2) Å, Al–N = 2.039 (2) Å) to which a Me$_2$AlCl molecule is coordinated through a (dative) Al–O bond of 1.895 (2) Å. The aluminum centers are four-coordinated with a distorted tetrahedral geometry. The chlorine atom is located in a semibridging position, but the long Al–Cl distance of 3.260 (1) Å is indicative for a nonbonding interaction. Enolate **3b'** crystallizes as pale yellow crystals in the space group $P2_1/n$ with a = 9.456 (1) Å, b = 14.145 (1) Å, c = 12.208 (1) Å, β = 103.78 (1)°, V = 1585.9 (2) Å^3, Z = 4, and T = 295 K. Full-matrix least-squares refinement on F converged at R = 0.051 and R_w = 0.043. The structures of enolates **3** and **3'** in solution as well as the reactions of these enolates with imines **4** is discussed. It is shown that both dimeric enolates **3** as well as monomeric adducts **3'** may act as the reactive intermediates in the one-pot synthesis of 3-amino-2-azetidinones **5** and **6**, which is characterized by the reactions of in situ prepared α-amino aluminum ester enolates with imines. Furthermore, on the basis of the structural features of **3b** and **3b'** the trans stereoselectivity, observed in these reactions, is explained in terms of two highly ordered transition states, constructed from *Z*-aluminum enolates and *E*-imines.

Introduction

Organometallic reagents derived from zinc and aluminum are important in organic synthesis for bringing about stereoselective carbon–carbon bond formation.[1] In recent years, selective carbon–carbon bond formation between a metallo ester enolate and an imine has become one of the major pathways for the preparation of β-lactam antibiotics.[2] Recently, we have found that substitution of the usually applied lithium cations for less electropositive zinc cations as counter-ions leads to α-amino zinc ester enolates, which react stereoselectively with imines to *trans*-3-amino-2-azetidinones.[3a-c] Subsequent studies on the influence of substituent and solvent effects on the stereoselectivity of these reactions indicated that the high trans stereoselectivity of these reactions is a result of the highly ordered transition state of the *Z*-zinc enolates with *E*-imines.[3d] This interpretation of the reaction course was supported by the first detailed structural study of the intermediate zinc enolates; e.g., the ethylzinc enolate of *N*,*N*-(*tert*-butyl, methyl)glycine methyl ester is tetrameric in the solid state, but in solution it is in equilibrium with a dimeric species.[4] The *Z* configuration of the enolate fragments in both the tetramer and the dimer is stabilized through intramolecular zinc–nitrogen coordination that is maintained in solution; accordingly, it is plausible to assume that the reactions of these zinc enolates with imines are chelation controlled.

As the first step in the reaction is the coordination of the imino nitrogen atom to the metal center, we next became interested in the application of α-amino aluminum ester enolates because of the different coordination properties of a R$_2$AlOR' fragment as compared to a RZnOR' fragment.

In general, little is known about the synthesis and structural features of aluminum enolates. A few reports on the application of aluminum enolates in the synthesis of β-lactams have appeared in the literature, although the intermediacy of aluminum enolates was not always recognized.[5]

† Debye Research Institute.
‡ Bijvoet Research Institute.

(1) See, for example (and ref 5): (a) Kitamura, M.; Suga, S.; Kawai, K.; Noyori, R. *J. Am. Chem. Soc.* **1986**, *108*, 6071. (b) Oguni, N.; Ohkawa, Y. *J. Chem. Soc., Chem. Commun.* **1988**, 1376. (c) Yamamoto, H.; Maruoka, K. *Pure Appl. Chem.* **1988**, *60*, 21. (d) Noyori, R. *Chem. Soc. Rev.* **1989**, *18*, 187.

(2) For recent reviews of the ester enolate–imine condensation, see: (a) Brown, M. J. *Heterocycles* **1989**, *29*, 2225. (b) Hart, D. J.; Ha., D.-C. *Chem. Rev.* **1989**, *89*, 1447. (c) van der Steen, F. H.; van Koten, G. *Tetrahedron* **1991**, in press.

(3) (a) van Vliet, M. R. P.; Jastrzebski, J. T. B. H.; Klaver, W. J.; Goubitz, K.; van Koten, G. *Recl. Trav. Chim. Pays-Bas* **1987**, *106*, 132. (b) Jastrzebski, J. T. B. H.; van der Steen, F. H.; van Koten, G. *Ibid.* **1987**, *106*, 516. (c) van der Steen, F. H.; Jastrzebski, J. T. B. H.; van Koten, G. *Tetrahedron Lett.* **1988**, *29*, 2467. (d) van der Steen, F. H.; Kleijn, H.; Jastrzebski, J. T. B. H.; van Koten, G. *Ibid.* **1989**, *30*, 765.

(4) (a) van der Steen, F. H.; Boersma, J.; Spek, A. L.; van Koten, G. *J. Organomet. Chem.* **1990**, *390*, C21. (b) van der Steen, F. H.; Boersma, J.; Spek, A. L.; van Koten, G. *Organometallics*, in press.

(5) (a) Liebeskind, L. S.; Welker, M. E.; Fengl, R. W. *J. Am. Chem. Soc.* **1986**, *108*, 6328. (b) Oguni, N.; Tomago, S.; Inami, K. *Chem. Express* **1986**, *1*, 579. (c) Wada, M.; Aiura, H.; Akiba, K. *Tetrahedron Lett.* **1987**, *28*, 3377. (d) Iwasaka, G.; Shibasaki, M. *Ibid.* **1987**, *28*, 3257. (e) Andreoli, P.; Cainelli, G.; Contento, M.; Giacomini, D.; Martelli, G.; Panunzio, M. *Ibid.* **1986**, *27*, 1695. (f) Cainelli, G.; Giacomini, D.; Panunzio, M.; Martelli, G.; Spunta, G. *Ibid.* **1987**, *28*, 5369. (g) Andreoli, P.; Cainelli, G.; Contento, M.; Giacomini, D.; Martelli, G.; Panunzio, M. *J. Chem. Soc., Perkin Trans. 1* **1988**, 945.

0002-7863/91/1513-5742$02.50/0

Table I. Synthesis of 3-Amino-2-azetidinones **5** via in Situ Prepared α-Amino Dialkylaluminum Ester Enolates (**3**)

entry	R	x[a]	R^1	R^2	product, yield[b] (%)	cis:trans[c]
1	Et	1.0	Ph	Me	**5a**, 45	10:90
2	Et	2.0	Ph	Me	**5a**, 96	8:92
3	Et	1.0	Ph	$SiMe_3/H$[d]	**5b**, 48	13:87
4	Et	2.0	Ph	$SiMe_3/H$[d]	**5b**, 94	10:90
5	Et	2.0	Me	CH_2Ph	**5c**, 96	<5:>95[e]
6	Me	1.2	2-furyl	$SiMe_3$	**5d**, 87	4:96

[a] Represents the R_2AlCl–Li enolate ratio. [b] Yields of the isolated crude products. [c] As determined by ^1H NMR integration of the characteristic proton signals of the crude products. [d] Upon hydrolysis, the protecting $SiMe_3$ group is replaced by a proton. [e] The cis isomer was not detected by ^1H NMR spectroscopy.

In this paper, we report the first results concerning a study of the synthesis, structural characterization, and reactivity toward simple imines of α-amino aluminum ester enolates.

To the best of our knowledge, this combined structure/reactivity study is the first to be reported in aluminum enolate chemistry.

Results

Synthesis of *trans*-3-Amino-2-azetidinones via Dialkylaluminum Enolates of *N,N*-Disubstituted Glycine Esters. As the primary aim of the present investigations was to establish whether α-amino aluminum ester enolates are suitable reagents for the stereoselective synthesis of *trans*-3-amino-2-azetidinones, only a limited set of both aluminum reagents and imines has been studied. Moreover, as 2-azetidinones **5** containing a free amino function at the 3-position are synthetically the most interesting products, most of the reactions were conducted with *N,N*-disilyl-protected α-amino ester enolates.

Accordingly, the reactions of the in situ prepared aluminum enolate **3a** of 2,2,5,5-tetramethyl-1-aza-2,5-disilacyclopentyl-1-acetic acid ethyl ester (**1a**)[6a] with several imines **4** were studied (eq 1). The results are summarized in Table I.

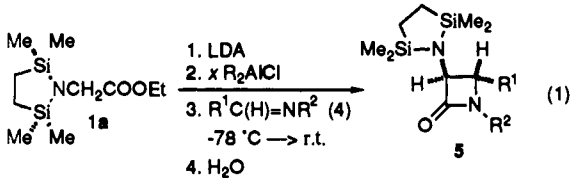

(1)

trans-2-Azetidinones **5a–d**, still containing the amino-protecting disilyl moiety, were synthesized in high yields, provided that a more than stoichiometric amount of dialkylaluminum chloride was used. When exactly (or slightly less than) 1 equiv of dialkylaluminum chloride was used, the 2-azetidinones **5** were obtained in moderate yields only (entries 1 and 3). The trans stereoselectivity of the reactions is good and comparable with the stereoselectivities observed for the reactions of the corresponding zinc enolate with the same imines.[3c,4]

In order to study the reactions of the dialkylaluminum enolates **3** with imines in more detail and to enable a comparison of their reactivity with that of the corresponding zinc enolates, several reactions of the in situ prepared lithium enolates **2b** and **2c** with *N*-benzylidenemethylamine (**4a**) were carried out in the presence of different amounts of dialkylaluminum chloride (eq 2). The results of these experiments are given in Table II.

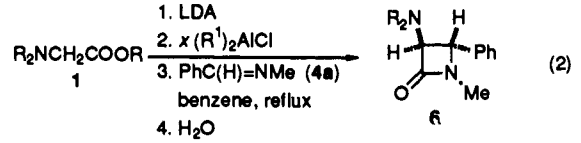

(2)

(6) (a) Overman et al. were the first who reported about the use of the lithium enolate of ester **1a** in the synthesis of 3-amino-2-azetidinones: Overman, L. E.; Osawa, T. *J. Am. Chem. Soc.* **1985**, *107*, 1698. (b) Jastrzebski, J. T. B. H.; van Koten, G.; van de Mieroop, W. F. *Inorg. Chim. Acta* **1988**, *142*, 169.

Table II. Reactions of $LiO(RO)C{=}C(H)NR_2$ (**2b**, R = Me; **2c**, R = Et) with $PhC(H){=}NMe$ (**4a**) in the Presence of Different Amounts of $(R^1)_2AlCl$

entry	R	R^1	x[a]	**6**, yield[b] (%)	cis:trans[c]	**7**, yield[b] (%)
1	Me	Me	0.25	**a**, 20	65:35	**a**, 4
2	Me	Me	0.8	**a**, 65	65:35	**a**, 17
3	Me	Me	1.0	**a**, 74	7:93	**a**, 8
4	Me	Me	1.2	**a**, 78	7:93	**a**, 8
5	Me	Me	2.0	**a**, 91	14:86	**a**, 2
6	Et	Me	0.8	**b**, 40	30:70	**b**, 15
7	Et	Me	1.0	**b**, 85	5:95	**b**, 5
8	Et	Et	1.0	**b**, 46	25:75	**b**, 9
9	Et	Me	1.2	**b**, 87	4:96	**b**, 2
10	Et	Me	2.0	**b**, 92	5:95	**b**, <2[d]
11	Et	Et	2.0	**b**, 84	5:95	**b**, <2[d]

[a] Represents the $(R^1)_2AlCl$–Li enolate ratio. [b] Yields of the isolated crude products, based on the amount of starting esters **1**. [c] As determined by ^1H NMR integration of the characteristic proton signals. [d] Not observed with ^1H NMR spectroscopy.

Scheme I

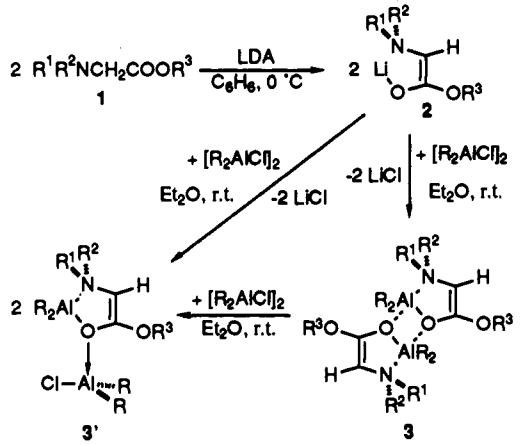

3b: R = R^1 = R^2 = R^3 = Me
3c: R = R^1 = R^2 = R^3 = Et
3d: R = R^1 = R^2 = Et, R^3 = *t*-Bu
3e: R = R^1 = R^3 = Me, R^2 = *t*-Bu

Surprisingly, besides the expected 2-azetidinones **6**, minor amounts of side products were formed. These were identified (NMR, GC–MS) as the amides $R_2NCH_2C(O)N(i\text{-}Pr)_2$ **7**. These amides may be formed by a reaction of diisopropylamine or -amide with either glycine esters **1** or with lithium **2** or aluminum enolates **3** (see Discussion).

The yield of **7** is dependent on the amount of added dialkylaluminum chloride. Furthermore, it appeared that the amount of added dialkylaluminum chloride also has a great influence on both the stereochemistry and the yields of the reactions affording 2-azetidinones **6**. Good yields of **6** with a high trans stereoselectivity are obtained when more than 1 mol equiv of dialkylaluminum chloride is used, and already a slight excess (>1 equiv) is sufficient to obtain good results. These observations strongly suggest that, depending on the amount of added dialkylaluminum chloride, species with a different reactivity are formed in solution (vide infra).

Synthesis of Dialkylaluminum Enolates $R_2AlO(R^2O)C{=}C(H)N(R^1)_2$ (3) and Their Dialkylaluminum Chloride Adducts $R_2AlO[(R^2O)C{=}C(H)N(R^1)_2]{\rightarrow}Al(Cl)R_2$ (3'). Stable dialkylaluminum enolates of N,N-disubstituted glycine esters **1** were synthesized as outlined in Scheme I.

As we have reported previously, lithium enolates **2** are easily prepared by deprotonation of esters **1** with lithium diisopropylamide.[4b,6b] Transmetalation of **2** with 1 equiv of dialkylaluminum chloride afforded organoaluminum enolates **3** in quantitative yields. Although the transmetalation may be carried out without isolation

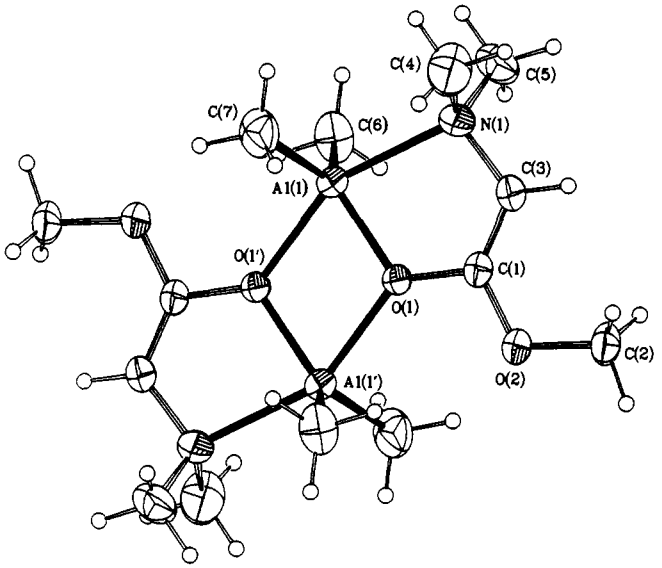

Figure 1. An ORTEP drawing (30% probability level) of the molecular structure of $[Me_2AlO(MeO)C{=}C(H)NMe_2]_2$ (**3b**), together with the adopted numbering scheme.

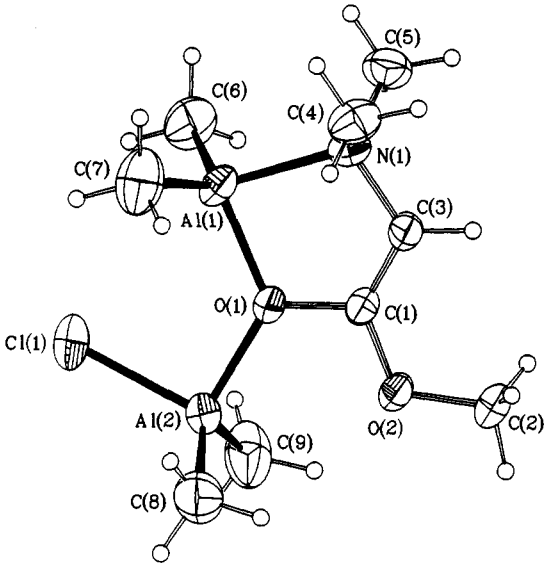

Figure 2. An ORTEP drawing (40% probability level) of the molecular structure of the coordination complex (**3b'**) of $Me_2AlO(MeO)C{=}C(H)NMe_2$ with Me_2AlCl, together with the adopted numbering scheme.

of **2**, aluminum enolates **3** of a higher purity are obtained when purified lithium enolates **2** are used.

Organoaluminum enolates **3** are very soluble in most organic solvents and extremely sensitive toward oxygen and moisture. Unfortunately, in most cases oily products were obtained, which were difficult to purify and characterize. Only **3b** was obtained as a solid and crystallized easily from diethyl ether at −30 °C. Cryoscopic molecular weight measurements showed that **3b** exists as a dimeric associate in benzene (c = 0.08 to 0.3 M). An X-ray structure determination of **3b** showed a dimeric structure in the solid state as well (vide infra).

When the transmetalation of **2** was carried out with 2 equiv of dialkylaluminum chloride or when 1 equiv of dialkylaluminum chloride was added to **3**, stable dialkylaluminum chloride–aluminum enolate adducts **3'** were obtained. Again, most adducts **3'** were isolated as extremely air-sensitive oils, but **3b'** and **3e'** were isolated as solids. ^1H and ^{13}C NMR spectroscopy of **3b'** showed the presence of two different resonances for the dialkylaluminum groups at room temperature, indicating that two different aluminum centers are present in the adduct. Cryoscopic molecular weight measurements of **3b'** in benzene correlated well with the monomeric dinuclear structure shown in Scheme I that was independently confirmed by an X-ray analysis (vide infra).

Both type of enolates, **3** and **3'**, are stable at room temperature; after storage in an inert atmosphere for several months no traces of decomposition or self-condensation products could be detected by NRM spectroscopy. Moreover, toluene solutions of **3** and **3'** can be heated for hours without any observable (^1H NMR) decomposition.

Molecular Structures of $[Me_2AlO(MeO)C{=}C(H)NMe_2]_2$ (3b) and $Me_2AlO[(MeO)C{=}C(H)NMe_2]{\rightarrow}Al(Cl)Me_2$ (3b'). Suitable single crystals of both **3b** and **3b'** were grown from solutions of these compounds in toluene at −30 °C. Crystals of **3b** are monoclinic and the unit cell contains two dimeric units. Crystals of **3b'** are likewise monoclinic but in this case the unit cell contains four monomeric dinuclear units. Figures 1 and 2 present views of the molecules, while selected bond distance and angles for both **3b** and **3b'** are listed in Table III.

As a result of intramolecular Al–N coordination in both **3b** and **3b'**, the enolate anions are N,O-chelate bound to a metal center, forming planar five-membered AlOCCN chelate rings. The configuration of the enolates is, as expected, Z. This type of chelation has also been observed for $[EtZnO(MeO)C{=}C(H)N(t\text{-}Bu)Me]_4$ (**8**),[4b] $[i\text{-}Bu_2AlOCH_2\text{-}2\text{-}C_5H_4N]_2$ (**9**),[7a] and $[Me_2AlO(Ph)CHCH(Me)N(H)Me]_2$ (**10**).[8]

Table III. Selected Bond Lengths (Å) and Angles (deg) with esd's in Parentheses for $[Me_2AlO(MeO)C{=}C(H)NMe_2]_2$ (**3b**) and $Me_2AlO[(MeO)C{=}C(H)NMe_2]{\rightarrow}Al(Cl)Me_2$ (**3b'**)

$[Me_2AlO(MeO)C{=}C(H)NMe_2]_2$ (**3b**)

Al(1)–O(1)	1.853 (3)	Al(1)–O(1')	2.055 (3)	Al(1)–N(1)	2.260 (3)
Al(1)–C(6)	1.952 (5)	Al(1)–C(7)	1.950 (5)	O(1)–C(1)	1.332 (5)
O(2)–C(1)	1.348 (4)	O(2)–C(2)	1.425 (5)	N(1)–C(3)	1.434 (5)
N(1)–C(4)	1.473 (5)	N(1)–C(5)	1.492 (6)	C(1)–C(3)	1.308 (6)

O(1)–Al(1)–O(1')	73.0 (1)	O(1)–Al(1)–N(1)	79.6 (1)
O(1)–Al(1)–C(6)	119.8 (2)	O(1)–Al(1)–C(7)	117.1 (2)
O(1')–Al(1)–N(1)	152.6 (1)	O(1')–Al(1)–C(6)	96.0 (2)
O(1')–Al(1)–C(7)	95.9 (2)	N(1)–Al(1)–C(6)	97.5 (2)
N(1)–Al(1)–C(7)	96.6 (2)	C(6)–Al(1)–C(7)	122.9 (2)
Al(1)–O(1)–Al(1')	107.0 (1)	Al(1)–O(1)–C(1)	118.7 (2)
Al(1')–O(1)–C(1)	134.3 (2)	Al(1)–N(1)–C(3)	103.6 (2)
Al(1)–N(1)–C(4)	113.7 (3)	Al(1)–N(1)–C(5)	114.0 (2)
O(1)–C(1)–O(2)	111.3 (3)	O(1)–C(1)–C(3)	121.3 (3)
O(2)–C(1)–C(3)	127.3 (3)	N(1)–C(3)–C(1)	116.7 (3)

$Me_2AlO[(MeO)C{=}C(H)NMe_2]{\rightarrow}Al(Cl)Me_2$ (**3b'**)

Al(1)···Cl(1)	3.260 (1)	Al(1)–O(1)	1.870 (2)	Al(1)–N(1)	2.039 (2)
Al(1)–C(6)	1.938 (4)	Al(1)–C(7)	1.929 (4)	Al(2)–Cl(1)	2.179 (1)
Al(2)–O(1)	1.895 (2)	Al(2)–C(8)	1.930 (5)	Al(2)–C(9)	1.949 (4)
O(1)–C(1)	1.360 (3)	O(2)–C(1)	1.338 (3)	O(2)–C(2)	1.429 (4)
N(1)–C(3)	1.450 (4)	N(1)–C(4)	1.492 (4)	N(1)–C(5)	1.498 (4)
C(1)–C(3)	1.306 (4)				

O(1)–Al(1)–N(1)	85.65 (9)	O(1)–Al(1)–C(6)	111.1 (1)
O(1)–Al(1)–C(7)	112.7 (2)	N(1)–Al(1)–C(6)	108.2 (2)
N(1)–Al(1)–C(7)	108.1 (2)	C(6)–Al(1)–C(7)	124.0 (2)
Cl(1)–Al(2)–O(1)	94.61 (7)	Cl(1)–Al(2)–C(8)	110.4 (1)
Cl(1)–Al(2)–C(9)	109.1 (2)	O(1)–Al(2)–C(8)	107.7 (2)
O(1)–Al(2)–C(9)	109.3 (1)	C(8)–Al(2)–C(9)	122.2 (2)
Al(1)–O(1)–Al(2)	126.6 (1)	Al(1)–O(1)–C(1)	111.8 (2)
Al(2)–O(1)–C(1)	121.6 (2)	Al(1)–N(1)–C(3)	104.8 (2)
Al(1)–N(1)–C(4)	112.5 (2)	Al(1)–N(1)–C(5)	113.0 (2)
O(1)–C(1)–O(2)	110.1 (2)	O(1)–C(1)–C(3)	120.6 (3)
O(2)–C(1)–C(3)	129.3 (3)	N(1)–C(3)–C(1)	117.0 (3)

Enolate **3b** has a dimeric structure; the two metal enolate fragments are related to each other by a center of symmetry as

(7) (a) van Vliet, M. R. P.; Buysingh, P.; van Koten, G.; Vrieze, K.; Kojić-Prodić, B.; Spek, A. L. *Organometallics* **1985**, *4*, 1701. (b) van Vliet, M. R. P.; van Koten, G.; Rotteveel, M. A.; Schrap, M.; Vrieze, K.; Kojic-Prodic, B.; Spek, A. L.; Duisenberg, A. J. M. *Ibid.* **1986**, *5*, 1389. (c) van Vliet, M. R. P.; van Koten, G.; de Keijser, M. S.; Buysingh, P.; Vrieze, K. *Ibid.* **1987**, *6*, 1652.

(8) Sierra, M. L.; de Mel, V. S. V.; Oliver, J. P. *Organometallics* **1989**, *8*, 2486.

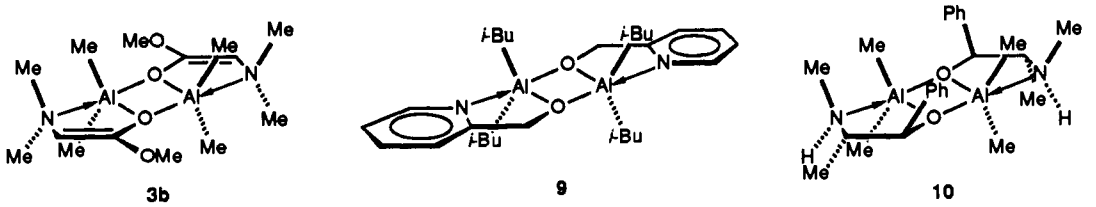

Figure 3. Schematic representations of the solid-state structures of five-coordinated organoaluminum compounds with a trigonal bipyramidal geometry around aluminum.

Table IV. Geometrical Data[a] of the Coordination Geometry around the Aluminum Atoms in Structurally Characterized Five-Coordinated Diorganoaluminum Compounds

compd	3b	9	10
Al–N	2.260 (3)	2.130 (5)	2.193 (8)
Al–O′	2.055 (3)	1.935 (5)	1.946 (7)
Al–O	1.853 (3)	1.853 (5)	1.864 (6)
Al–C	1.950 (5)	1.974 (6)	1.989 (9)
	1.952 (5)	2.014 (6)	1.999 (8)
N–Al–O′	152.6 (1)	151.7 (2)	151.6 (3)
N–Al–O	79.6 (1)	77.7 (2)	78.5 (3)

[a] Bond lengths in angstroms and angles in degrees.

found for both **9** and **10**. The oxygen atom of one enolate fragment is coordinated to the aluminum atom of a second enolate fragment, forming a central Al_2O_2 ring with an Al(1)–O(1) bond of 1.853 (3) Å and a longer Al(1)–O(1′) coordination bond of 2.055 (3) Å. As a result of Al(1)–N(1) coordination the aluminum centers are five-coordinated with a distorted trigonal bipyramidal geometry. Analysis of the coordination-sphere around aluminum in **3b** according to a model developed by Holmes[9] showed the character of the geometry to be ca. 80% trigonal bipyramidal. The aluminum atom lies well within the equatorial plane that is defined by O(1), C(6), and C(7). In this plane, the values of the three angles subtended at aluminum are all close to the ideal value of 120° (117.1 (2)–122.9 (2)°), indicating only a minor distortion of the trigonal bipyramidal geometry. However, the value of the angle defined by the two apical substituents, O(1′) and N(1), lies far from the ideal value of 180° (152.6 (1)°). This distortion is likely caused by ring strain in both the five-membered AlOCCN chelate ring and the four-membered Al_2O_2 ring.

Structurally characterized five-coordinated organoaluminum compounds with a trigonal bipyramidal geometry around aluminum are quite rare and only two other solid-state structures, **9** and **10**, wherein the apical positions of the trigonal bipyramid are occupied by a nitrogen and oxygen atom, have been reported.[7a,8] The geometrical data of the coordination sphere in **3b** and these compounds are summarized in Table IV.

In all three structures two carbon atoms and one oxygen atom lie in the equatorial plane. The longer Al–X distances for the apical atoms in **3b** compared to those in **9** and **10** are most likely caused by steric repulsions (see Figure 3). Because of these long Al–X bonds, the bonds of the aluminum atom with the atoms in the equatorial plane should be slightly contracted since the aluminum center becomes more electrophilic. This is indeed the case for the Al–C carbon bonds that in **3b** are ca. 0.04 Å shorter than the Al–C bonds in **9** and **10**. However, the equatorial Al–O bond lengths are virtually the same in all three compounds. This contrasts with the marked change of Zn–O distances when going from a β-amino alcoholate (1.98 (1) and 2.06 (1) Å)[10] to an α-amino enolate (2.02 (1) and 2.12 (1) Å)[11] and finally an α-amino ester enolate (average 2.032 (2) and 2.065 (4) Å).[4] In our opinion, in these organozinc–chelate complexes the hybridization of the oxygen atom of the chelating ligand and consequently the character of the Zn–O bonds changes from sp^3 to sp^2.[4] However, the trigonal bipyramidal geometry of the aluminum atoms in **3b**, **9**, and **10** results in almost completely planar basic molecular frames, and therefore these structures all contain sp^2-hybridized bridging oxygen atoms. That the Al–O bond lengths are the same in **3b**, **9**, and **10** may be explained by the fact that in **3b** the electron density is partly delocalized, as is indicated by the relatively short O(1)–C(1) and long C(1)=C(3) bond lengths of 1.332 (5) and 1.308 (6) Å, respectively. Such a delocalization was also observed for ethylzinc ester enolate **8**, wherein these bond lengths (average) are 1.314 (6) and 1.327 (7) Å, respectively,[4] but not observed for (*unreactive*) $[EtZnO(Me)C{=}C(H)N(t\text{-}Bu)Et]_2$, wherein these bond lengths are 1.40 (2) and 1.27 (3) Å, respectively.[11] As a result of this delocalization the electron density on, and hence the Lewis basicity of, O(1) in **3b** is less than in **9** and **10**. Consequently, a longer equatorial Al–O bond is expected to be found in **3b**. However, because of the previously mentioned enhanced electrophilicity of the aluminum atom in **3b**, the Al–O bond is slightly contracted resulting in a bond length that is comparable with those in **9** and **10**.

Enolate **3b′** has a monomeric, dinuclear structure and is the first example of a Me_2AlCl adduct of a metal ester enolate. The complex consists of a mononuclear unit of **3b** to which a Me_2AlCl molecule is attached through coordination of the enolato-oxygen to the aluminum of Me_2AlCl. To our knowledge, the only other structurally characterized dinuclear organoaluminum species (with coordinated trimethylaluminum) reported are $Me_2AlO[C(Me)_2C(H){=}N(t\text{-}Bu)]{\rightarrow}AlMe_3$ (**11**),[7b] $Me_2AlO[C(H)(Me)N(Ph)C(Ph){=}O]{\rightarrow}AlMe_3$ (**12**),[12] and $Me_2AlO[N(Me)NO]{\rightarrow}AlMe_3$ (**13**).[13] In all these dinuclear complexes the aluminum centers are four-coordinated with a distorted tetrahedral surrounding. The geometrical data of the enolate fragment in **3b′** are quite similar to those found in **3b**. The distances of Al(1) to C(6), C(7), and N(1) in **3b′** are shorter than the same distances in **3b** because the tetrahedral surrounding of aluminum allows better orbital overlap than a trigonal bipyramidal surrounding. Furthermore, the steric repulsions between the methyl groups attached to aluminum and nitrogen are, because of the tetrahedral surrounding, in **3b′** much less than in **3b**, which accounts for the large difference observed for the dative Al–N bonds in **3b** (2.260 (3) Å) and in **3b′** (2.039 (2) Å). The Al(1)–O(1) bond of 1.870 (2) Å in **3b′** is longer than the Al(1)–O(1) bond of 1.853 (3) Å in **3b**. This is the result of the lower Lewis basicity of O(1) in **3b′** because of a strong interaction with the very Lewis acidic aluminum atom of Me_2AlCl (Al(2)–O(1) = 1.895 (2) Å).

The atoms of the chelate ring as well as both the aluminum and chlorine atoms all lie within one plane. The chlorine atom of the Me_2AlCl unit is directed to Al(1), as indicated by a O(1)–Al(2)–Cl(1) angle of 94.61 (7)°, which lies far from the ideal tetrahedral value. Nevertheless, the Al(1)–Cl(1) distance of 3.260 (1) Å is obviously too long for a significant bonding interaction. In the other dinuclear organoaluminum structures **11**–**13**, the tetrahedral geometry of the coordinated trimethylaluminum molecule is retained better and the methyl groups closest to the second aluminum center do not lie perfectly in the plane defined by the two aluminum centers and the bridging oxygen atom as would be expected when a certain amount of interaction between

(9) Holmes, R. R. *Prog. Inorg. Chem.* **1984**, *32*, 119.
(10) Kitamura, M.; Okada, S.; Suga, S.; Noyori, R. *J. Am. Chem. Soc.* **1989**, *111*, 4028.
(11) van Vliet, M. R. P.; van Koten, G.; Buysingh, P.; Jastrzebski, J. T. B. H.; Spek, A. L. *Organometallics* **1987**, *6*, 537.
(12) Kai, Y.; Yasuoka, N.; Kasai, N.; Kakudo, M. *Bull. Chem. Soc. Jpn.* **1972**, *45*, 3403.
(13) Amirkhalili, S.; Hitchcock, P. B.; Smith, J. D.; Stamper, J. G. *J. Chem. Soc., Dalton Trans.* **1980**, 2493.

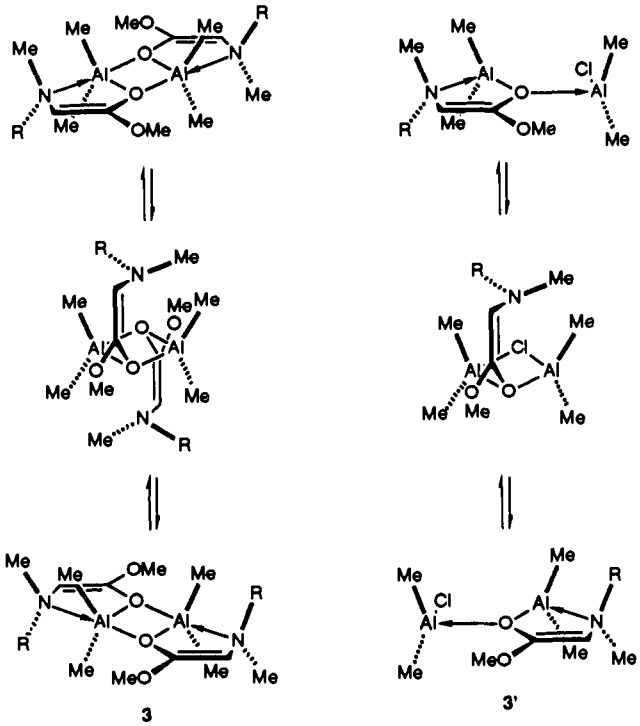

Figure 4. Schematic representations of the exchange processes involving Al–N coordination/decoordination in both dimeric **3** and monomeric, dinuclear organoaluminum enolates **3′**.

Al(1) and a methyl group would be present.

Dynamic Behavior in Solution of Aluminum Enolates 3 and Adducts 3′ and Their Reactivity toward *N*-benzylidenemethylamine (4a). Compounds **3b** and **3e** and their dimethylaluminum chloride adducts **3b′** and **3e′** were used as model compounds to study their dynamic behavior in solution.

Enolate **3b** has a perfectly symmetrical arrangement and contains no stereogenic centers; therefore, a dynamic process like Al–N coordination/decoordination cannot be detected by NMR. However, enolate **3e** contains a prochiral amino nitrogen atom that upon coordination to the aluminum atom becomes a stable chiral center, and the two aluminum-bound methyl groups are then inequivalent. At room temperature all resonances in the ^1H NMR spectrum appear as singlets, but at 253 K the signal of the two aluminum-bound methyl groups is resolved in two single resonances. This indicates that at 253 K the Al–N dissociation process is slow on the NMR time scale. The energy of activation (ΔE_a) for the Al–N dissociation was determined to be 13.6 kcal/mol by standard line-shape analysis.

The ^1H and ^{13}C NMR spectra of adduct **3b′** show two single resonances for the methyl groups of the two aluminum centers when recorded at room temperature. When the solution is heated to 318 K they coalesce to a single resonance. This implies that the chemical surrounding of both aluminum centers has become equivalent, most likely through a rapid exchange process as shown in Figure 4. The energy of activation for this process was determined to be 16.0 kcal/mol by standard line-shape analysis.

The room-temperature ^1H and ^{13}C NMR spectra of adduct **3e′** show three resonances with relative intensities of 1:2:1 for the methyl groups of the two aluminum centers. Apparently, at that temperature the Al–N coordination is stable on the NMR time scale, resulting in two inequivalent aluminum-bound methyl groups. At 313 K, all these groups appear as a single, broad resonance. This indicates that the Al–N coordination is lost and the two aluminum centers have become equivalent (ΔE_a = 15.6 kcal/mol).

Both the dimeric enolate **3b** and the adduct **3b′** react quantitatively with imine **4a**, yielding *trans*-1-methyl-3-(dimethylamino)-4-phenyl-2-azetidinone **6a** (eq 3). Monitoring of these reactions by ^1H NMR spectroscopy revealed that adduct **3b′** is slightly more reactive than dimeric **3b**. After 1 h at room temperature, 30% of **3b′** is converted into **6a**, whereas for **3b** only trace amounts of **6a** are found. Furthermore, after 5 min at 80 °C, **3b′** is completely converted into **6a**, whereas 10 min at 80 °C are required for a full conversion of **3b**.

Scheme II[a]

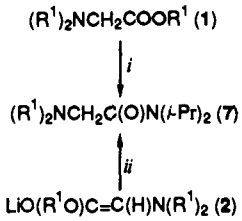

[a] Key: i, **a** $Me_2AlN(i\text{-}Pr)_2$ (<5% yield of **7**), **b** $Me_2AlCl{\cdot}HN(i\text{-}Pr)_2$ (<2% yield of **7**), **c** $Me_3Al/HN(i\text{-}Pr)_2$ (<2% yield of **7**); ii, **d** $Me_2AlN(i\text{-}Pr)_2$ (<2% yield of **7**), **e** $Me_2AlCl{\cdot}HN(i\text{-}Pr)_2$ (25% yield of **7**).

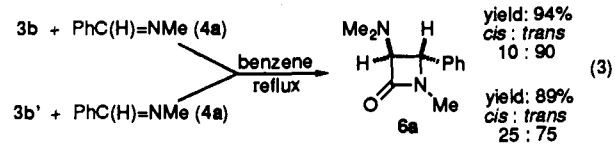

The trans stereoselectivity of the reaction of dimeric **3b** with **4a** is significantly better than that of the reaction of monomeric dinuclear **3b′**. This is most likely the result of different steric demands of the enolates in the transition state (vide infra). Quite surprisingly, the stereoselectivity of the reaction of pure dinuclear adduct **3b′** with imine **4a** is enhanced in the presence of diisopropylamine, affording *trans*-1-methyl-3-(dimethylamino)-4-phenyl-2-azetidinone **6a** with a de of 90%, whereas in the absence of diisopropylamine the de is only 50%. This increased stereoselectivity is not observed for the reaction of dimeric **3b** with imine **4a** that affords *trans*-**6a** with a de of 84% in the presence of diisopropylamine and of 80% in the absence of diisopropylamine. Dimeric **3b** has no space available to accomodate the bulky diisopropylamine, whereas adduct **3b′** has a more open structure, containing four-coordinated aluminum centers that are perfectly capable to coordinate diisopropylamine as an extra ligand. Owing to this coordination, the structures and hence the relative energies of the transition states (vide infra) are changed.

Discussion

Aspects of the Application of α-Amino Aluminum Ester Enolates in the Synthesis of 3-Amino-2-azetidinones. In situ prepared α-amino aluminum ester enolates are successfully applied in the synthesis of 3-amino-2-azetidinones **5** and **6**. However, high yields of **5** and **6** are only obtained when a small excess of dialkylaluminum chloride is used for the transmetalation of the parent lithium enolates. The trans stereoselectivities observed in the reactions leading to protected 3-amino-2-azetidinones **5** are in good agreement with those observed in the same reactions with the corresponding zinc enolate.[3] However, for the dialkylamino aluminum ester enolates an increase in trans stereoselectivity is observed compared to the results obtained for the same zinc enolates. For instance, for the zinc dichloride mediated reaction to 1-methyl-3-(dimethylamino)-4-phenyl-2-azetidinone **6b** no stereoselectivity was obtained,[3] whereas the dialkylaluminum chloride mediated reaction results in a de of 72–86%, depending on the amount of dialkylaluminum chloride used. This increased stereoselectivity can be ascribed to the fact that in the case of the zinc-mediated reactions the transition state is formed around a tetrahedrally surrounded metal center, whereas for the aluminum-mediated reactions the metal center has a trigonal bipyramidal surrounding (vide infra).

Unfortunately, the dialkylaluminum chloride mediated reactions are not as clean as the zinc-mediated reactions, because along with the 2-azetidinones **6** some minor amounts of amides **7** are formed. These amides may be formed via various pathways as indicated in Scheme II.

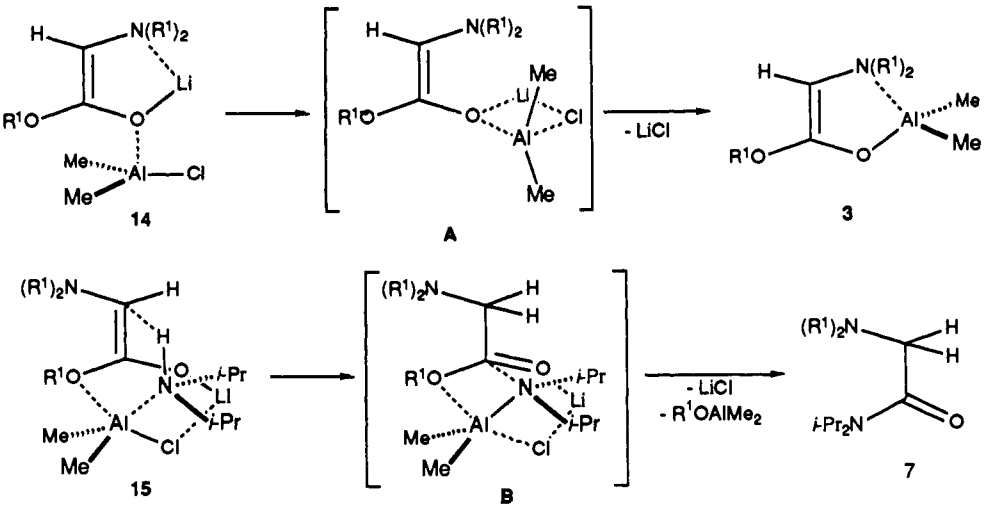

Figure 5. Schematic representations of the mechanism of the transmetalation of lithium enolates **2** with Me_2AlCl and of the formation of the amides **7** accompanying this transmetalation.

These pathways were investigated in detail for amide **7a** (R^1 = Me). Obviously, amides **7** are not formed directly from the free esters **1**, since reactions of **1** with aluminum amide (a) or aluminum amine (b) afforded no amide **7a** at all. In situ generated aluminum amide (c) also did not afford amide **7a**, although it is a known literature procedure to convert esters in tertiary amides.[14] The reaction of lithium enolate **2b** with aluminum amide (d) also did not yield amide **7a** either. Surprisingly, with aluminum amine (e), amide **7a** was formed in 25% yield. Clearly, the amides are formed during the transmetalation reaction. Indeed, when dimethylaluminum chloride was added to a solution of in situ prepared lithium enolate **2b**, i.e., in the presence of diisopropylamine, amide **7a** was isolated in 9% yield. A possible explanation for the appearance of this side reaction is depicted in Figure 5.

The top half of the figure shows our proposed mechanism of the transmetalation reaction, involving as the first step coordination of dimethylaluminum chloride to the enolato oxygen of a lithium enolate fragment.[15] In this figure, the lithium enolate is represented as a monomeric associate **14** with a *Z* configuration; the same line of reasoning holds true for the higher associates and enolates with an *E* configuration. The driving force for the transmetalation reaction is the formation of lithium chloride, most likely via a concerted mechanism (A) as shown in Figure 5. The bottom half of the figure shows our proposed mechanism for the formation of amides **7**. The diisopropylamine, which already may be present in the starting lithium enolate[16] or is provided by the aluminum compound, plays a crucial role. The configuration of the starting enolate is presumably *E*, because in the *Z*-enolate there is no room available for coordination of the bulky diisopropylamine. The presence of diisopropylamine causes the aluminum atom to coordinate to the alkoxy oxygen as shown in **15**. Presumably, the first step is the transfer of a proton from the amine to the enolate followed by elimination of dimethylaluminum alkoxide and subsequent formation of the amide via a concerted reaction (B).

Both reactions may occur simultaneously, and the fact that no amide **7** is formed when the transmetalation is carried out below −30 °C indicates that the rate of the transmetalation reaction is larger than that of the competitive amide formation reaction. Examination of the data given in Table II indicates that the amount of amide **7** decreases when the amount of added dialkylaluminum chloride is increased. This may be explained by

Scheme III

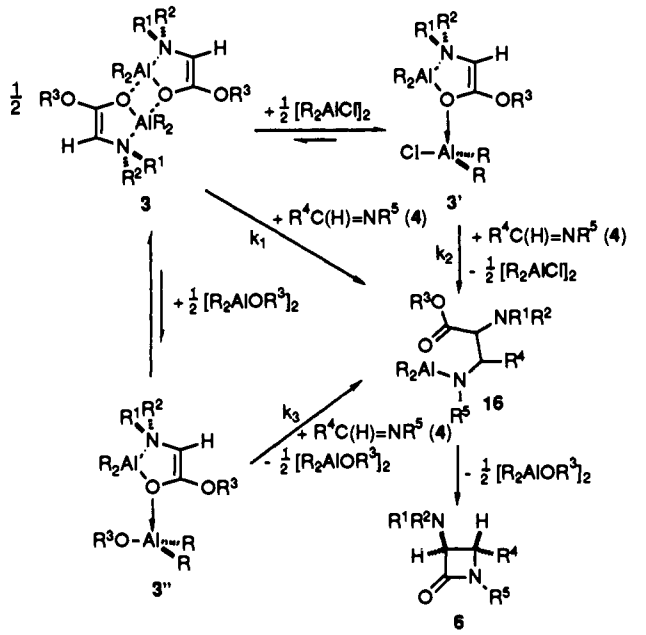

the fact that a second molecule of dimethylaluminum chloride can coordinate to the enolato oxygen in **15** (coming in from the back-side) and the resulting species may now react either via transition state A (affording enolate **3**) or via transition state B (affording amide **7**), which is reflected by an increased formation of enolate **3**.

Mechanistic and Stereochemical Aspects of the Reaction of α-Dialkylamino Dialkylaluminum Ester Enolates with Imines. The results obtained for the reactions of in situ prepared α-amino dialkylaluminum ester enolates indicate that more than 1 equiv of dialkylaluminum chloride is necessary for a quantitative conversion of the enolates to 2-azetidinones. The reaction sequence shown in Scheme III provides a plausible explanation.

When the transmetalation is carried out with 1 equiv of dialkylaluminum chloride, a dimeric enolate **3** is formed. This enolate then reacts with imine **4** to form an aldolate **16**. Ring closure and elimination of dialkylaluminum alkoxide affords 3-amino-2-azetidinone **6**. The liberated dialkylaluminum alkoxide can act as a (strong) Lewis acid to form a dinuclear complex **3″** that might be deactivated for further reaction with imine **4** (i.e., k_3 is very small). When more than 1 equiv of dialkylaluminum chloride is used, dimeric enolate **3** is (at least partly, depending on the amount of added dialkylaluminum chloride) cleaved into dinuclear complex **3′**. The coordinated dialkylaluminum chloride

(14) Basha, A.; Lipton, M.; Weinreb, M. *Tetrahedron Lett.* **1977**, *48*, 4171.

(15) In our opinion, transmetalation via a carbon-metalated species and subsequent shift of the metal to the enolate oxygen is less likely, but cannot be ruled out.

(16) Lithium enolates containing complexed secondary amines have been structurally characterized: Laube, T.; Dunitz, J. D.; Seebach, D. *Helv. Chim. Acta* **1985**, *68*, 1373.

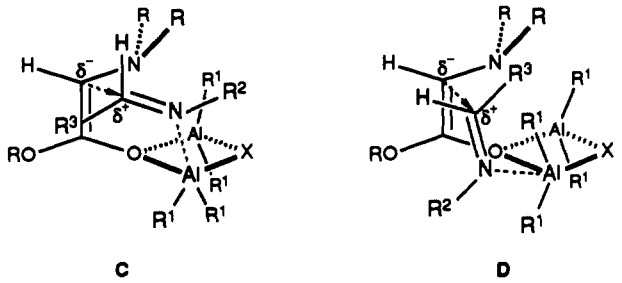

C D

Figure 6. Schematic representations of two transition states, constructed of a *Z*-aluminum enolate and an *E*-imine, that explain the formation of *trans*-2-azetidinones (via C) and *cis*-2-azetidinones (via D).

is not consumed during reaction with imine **4**, and after formation of 3-amino-2-azetidinone **6**, it can be used to cleave another molecule of dimeric enolate **3**. Since dialkylaluminum chloride is a better Lewis acid than dialkylaluminum alkoxide, the formation of adduct **3''** is now unlikely. The assumption that k_2 is larger than k_1 justifies the proposition that adduct **3'** is the actual species that reacts with imines **4**.

However, several observations are in contradiction with this proposed reaction scheme: (i) attempts to synthesize complex **3b''** by conproportionation of **3** with dimethylaluminum methoxide failed, and therefore it is unlikely that complexes **3''** are formed during the reactions of **3** to azetidinones **6**; (ii) the reaction of pure dimeric aluminum enolate **3b** with imine **4a** affords 2-azetidinone **6a** in almost quantitative yield; (iii) the rate of reaction observed for the pure adduct **3b'** with imine **4a** is only slightly larger than that observed for pure enolate **3b**; and (iv) the stereoselectivities observed for the reactions of in situ prepared aluminum enolates (see Table II) are closer to that observed for the reaction of pure enolate **3b** with imine **4a** than that of pure adduct **3b'**.

Therefore, we conclude that the role of the excess dialkylaluminum chloride added to lithium enolates **2** is to suppress the side reactions leading to amides **7** and that the reactions with imines **4** go mainly via dimeric enolates **3** and only for minor extend via adducts **3'**.

Hence, for the in situ preparation of azetidinones **6** both the dimeric enolates **3** as well as the dinuclear adducts **3'** can act as the reactive species. Because of the intramolecular Al–N coordination both types of enolates do have the *Z* configuration in the solid state (vide supra), and we have no reason to assume that this configuration is different in solution. The first step of the reactions with imines is cleavage of this Al–N coordination to create a free coordination site on the metal center (i.e., in dimeric enolates **3**), which is subsequently occupied by the nitrogen atom of the imine. This coordinated imine is then activated for a nucleophilic attack of the α-carbon atom of the enolate anion on the electrophilic imino carbon atom. The stereochemistry of the final 2-azetidinone product is determined during this C–C bond formation. Figure 6 displays two transition states, constructed from a *Z*-enolate and an *E*-imine, that we propose for this reaction (X = O(RO)C=C(H)NR_2 for dimeric enolates **3** and X = Cl for dinuclear adducts **3'**).

Transition state C results in an erythro C–C bond formation that leads to a *trans*-2-azetidinone and transition state D results in a threo C–C bond formation that leads to a *cis*-2-azetidinone. The energy difference between the two transition states is determined by the steric repulsions between substituents of the imine and the enolate. It is obvious that in transition state C these repulsions are less than in D and therefore the energy of activation for C will be lower than for D; i.e., the reaction of enolates **3** (or **3'**) with imines **4** will yield more of the *trans*-2-azetidinones **6**.[17]

(17) For a review on the stereochemistry of aldol-type reactions, the reader is referred to: Evans, D. A.; Nelson, J. V.; Taber, T. R. In *Topics in Stereochemistry*; Allinger, N. L., Eliel, E. L., Wilen, S. H., Eds.; Wiley-Interscience: New York, 1982; Vol. 13, p 1. A more detailed discussion about the stereochemistry of the reaction of α-amino ester enolates with imines will appear in *J. Org. Chem.*

Concluding Remarks

Reactions of in situ prepared dialkylaluminum enolates of N,N-disubstituted glycine esters **1** with simple imines **4** selectively afford *trans*-3-amino-2-azetidinones **5** and **6**. Excellent yields are obtained when an (small) excess of dialkylaluminum chloride is present.

The results of the reactions yielding protected 3-amino-2-azetidinones **5** differ little from those observed for our zinc-mediated route. However, for reactions to 3-amino-2-azetidinones **6** a considerable enhancement of the trans stereoselectivity is observed for the aluminum-mediated route. A disadvantage in the latter case is the formation of amides **7** as side products that are produced during the transmetalation step.

Pure α-amino dialkylaluminum ester enolates are easily prepared by transmetalation of lithium enolate precursors **2** with dialkylaluminum chloride. Depending on the amount of dialkylaluminum chloride added, two types of structures are formed: a dimeric enolate **3** and/or a monomeric dinuclear dialkylaluminum chloride adduct **3'**. In both types, the enolate anion is N,O-chelate bound to an aluminum atom and consequently has a *Z* configuration.

The high trans stereoselectivity observed for the reactions of α-amino aluminum ester enolates with imines can be explained by highly ordered transition states consisting of an *E*-imine that is coordinated to a *Z*-enolate.

Although more experimental data (especially about the kinetics of the reactions affording the 2-azetidinone products) are necessary to support our proposal for the structure of the active intermediates, the results presented in this paper indicate that both the dimeric enolates **3** and dinuclear adducts **3'** may be the active intermediates that react with imines.

Experimental Section

General Procedures. All manipulations were carried out under a dry, oxygen-free, nitrogen atmosphere using standard Schlenk techniques. Solvents were dried and distilled from sodium/benzophenone prior to use. ^1H and ^{13}C NMR spectra were recorded on a Bruker AC-200 or Varian EM-360 NMR spectrometer at 295 K, unless stated otherwise. Chemical shifts (δ) are in parts per million relative to Me_4Si as an external standard. Coupling constants are in hertz. Cryoscopic molecular weight determinations were performed in a home-made apparatus based on a design by Bauer and Seebach.[18] Elemental analyses were performed by the Institute of Applied Chemistry (TNO), Zeist, The Netherlands.[19]

N,N-(disubstituted) glycine esters (**1b–d**),[4b] 2,2,5,5-tetramethyl-1-aza-2,5-disila-cyclopentane-1-acetic acid ethyl ester (**1a**),[20] lithium enolates (**2b–d**),[4b] and imines (**4**)[21] were synthesized according to published methods. Solutions (1.0 M) of dimethyl- and diethylaluminum chloride in hexanes were purchased from Aldrich Chemical Co.

General Procedure for the One-Pot Synthesis of 3-(2,2,5,5-Tetramethyl-1-aza-2,5-disilacyclopentyl)-2-azetidinones (5). To a stirred solution containing *N,N*-diisopropylamine (1.01 g, 10 mmol) in 30 mL of solvent (diethyl ether or hexane) at −78 °C was added 10 mmol of *n*-butyllithium (6.67 mL of a 1.5 M solution in hexanes). The solution was stirred for 10 min at −78 °C, and then 10 mmol (2.45 g) of 2,2,5,5-tetramethyl-1-aza-2,5-disilacyclopentane-1-acetic acid ethyl ester **1a** was added. The reaction mixture was stirred for an additional 15 min at −78 °C, the appropriate amount of dialkylaluminum chloride (*x* mL of a 1.0 M solution in hexanes) was added by syringe, and after stirring for 0.5 h, 10 mmol of an appropriate imine was added at −78 °C. The reaction mixture was then stirred for 1 h at −78 °C, after which the reaction mixture was allowed to warm up to room temperature and quenched *carefully* with 20 mL of a saturated aqueous ammonium chloride solution. *Note*: the reaction mixture still contains alkylaluminum species that react *violently* or even explosively with water, and therefore the aqueous ammonium chloride solution is added *dropwise* until the evolution of alkanes is completed. The precipitated salts were filtered off through a sintered-glass fritt. The aqueous layer was sepa-

(18) Bauer, W.; Seebach, D. *Helv. Chim. Acta* **1984**, *67*, 1972.

(19) Elemental analysis of air-sensitive compounds containing volatile organic fragments always showed too low values for the C, H, and N analyses because of partial hydrolysis during sampling.

(20) Djuric, S.; Venit, J.; Magnus, P. *Tetrahedron Lett.* **1981**, *22*, 1787.

(21) (a) Patai, S. In *The Chemistry of the Carbon-Nitrogen Double Bond*; Patai, S., Ed.; Interscience: London 1970; pp 363–407. (b) Burnett, D. A.; Hart, D.; Liu, J. *J. Org. Chem.* **1986**, *51*, 1930.

rated and extracted with two portions of diethyl ether. The combined organic extracts were dried on sodium sulfate and concentrated in vacuo to afford the crude 2-azetidinone products **5**. The composition of these crude products was analyzed using ^{1}H NMR spectroscopy. The 2-azetidinones **5** were identified by comparison with authentic samples obtained by our zinc dichloride mediated route.[3]

General Procedure for the One-Pot Synthesis of 3-(*N*,*N*-(Disubstituted)amino)-2-azetidinones. To a stirred solution containing 1.01 g (10 mmol) of *N*,*N*-diisopropylamine in 30 mL of benzene or toluene was added 10 mmol of *n*-butyllithium (6.67 mL of a 1.5 M solution in hexanes). The resulting solution was stirred for 10 min, and then 10 mmol of a N,N-disubstituted glycine ester was added at 0 °C. The reaction mixture was stirred for an additional 15 min, and then the appropriate amount of dialkylaluminum chloride (x mL of a 1.0 M solution in hexanes) was added by syringe. After the mixture was stirred for 0.5 h at room temperature, 10 mmol of *N*-benzylidenemethylamine **4a** was added. Then, the reaction mixture was refluxed until no further formation of 2-azetidinone could be detected by ^{1}H NMR. The reaction mixture was allowed to cool to room temperature and then *carefully* (vide supra) quenched with 20 mL of a saturated aqueous ammonium chloride solution. The precipitated salts were filtered off through a sintered-glass fritt. The aqueous layer was separated and extracted with two portions of diethyl ether. The combined organic extracts were dried on sodium sulfate and concentrated in vacuo to afford the crude 2-azetidinone products **6**. The composition of these crude products was analyzed using ^{1}H NMR spectroscopy. The 2-azetidinones **6** were identified by comparison with authentic samples obtained by our zinc dichloride mediated route.[3]

$Me_2AlCl{\cdot}HN(i\text{-}Pr)_2$. To a stirred solution containing 0.51 g (5 mmol) of diisopropylamine in 15 mL of benzene was added 5 mmol of dimethylaluminum chloride (5.0 mL of a 1.0 M solution in hexanes) at room temperature. Evolution of methane was not observed, although a slightly exothermic reaction occurred. The clear solution was stirred overnight at room temperature and then concentrated in vacuo, yielding 1.93 g (99%) of pure $Me_2AlCl{\cdot}HN(i\text{-}Pr)_2$ as a white solid: ^{1}H NMR (benzene-d_6) δ 3.03 (d sept, 2 H, J = 6.7, N(C*H*(CH$_3$)$_2$)$_2$), 1.97 (br s, 1 H, N*H*), 0.78 and 0.73 (d, 6 H, J = 6.7, N(CH(C*H*$_3$)$_2$)$_2$), −0.22 (s, 6 H, Al(C*H*$_3$)$_2$).

$Me_2NCH_2C(O)N(i\text{-}Pr)_2$ (7a). The best yield of **7a** was obtained from the reaction of $Me_2AlCl{\cdot}HN(i\text{-}Pr)_2$ with LiO(MeO)C=C(H)NMe$_2$ (**2b**, see text). To a stirred suspension of 0.62 g (5 mmol) of **2b** in 30 mL of benzene was added 1.93 g (5 mmol) of $Me_2AlCl{\cdot}HN(i\text{-}Pr)_2$ in 25 mL of benzene. Immediately, a white precipitate (LiCl) was formed. The resulting pale yellow suspension was stirred for 4 h at 50 °C and then *carefully* (vide supra) quenched with 20 mL of a saturated aqueous ammonium chloride solution. The precipitated salts were filtered off through a sintered-glass fritt. The aqueous layer was separated and extracted with two portions of diethyl ether. The combined organic extracts were dried over sodium sulfate and concentrated in vacuo (at 35 °C (0.5 mmHg)) to afford pure **7a** as a pale yellow oil: ^{1}H NMR (benzene-d_6) δ 4.15 and 3.01 (sept, 1 H, J = 6.5, N(C*H*(CH$_3$)$_2$)$_2$), 2.89 (s, 2 H, NC*H*$_2$C(O)N), 2.05 (s, 6 H, N(C*H*$_3$)$_2$), 1.43 and 0.88 (d, 6 H, J = 6.5, N(CH(C*H*$_3$)$_2$)$_2$); ^{13}C NMR (benzene-d_6) δ 168.52 (*C*=O), 65.62 and 48.78 (N(*C*H(CH$_3$)$_2$)$_2$), 45.71 (N*C*H$_2$C(O)N), 45.23 (N(*C*H$_3$)$_2$), 20.64 (N(CH(*C*H$_3$)$_2$)$_2$; MS m/z 186 ($C_{10}H_{22}N_2O^+$, 3), 58 ($Me_2NCH_2^+$, 100); IR (KBr, Nujol) 2850, 1650, 1450, 1370.

General Procedure for the Synthesis of Dialkylaluminum Enolates 3. To a solution (or suspension) containing 10 mmol of a preformed lithium enolate of a N,N-disubstituted glycine ester in 50 mL of diethyl ether was added 10 mmol of a dialkylaluminum chloride (10.0 mL of a 1.0 M solution in hexanes) at 0 °C. Immediately, a white solid (LiCl) started to precipitate, and after stirring for 30 min at room temperature, the solid was removed by centrifugation and extracted twice with 30 mL of diethyl ether. The combined etheral extracts were concentrated in vacuo, affording the dialkylaluminum enolates **3** with physical data as follows.

$Me_2AlO(MeO)C{=}C(H)NMe_2$ (3b): off-white solid, isolated yield 98%; ^{1}H NMR (benzene-d_6) δ 3.82 (s, 1 H, *H*C=C), 3.12 (s, 3 H, OC*H*$_3$), 2.00 (s, 6 H, N(C*H*$_3$)$_2$), −0.31 (s, 6 H, Al(C*H*$_3$)$_2$); ^{13}C NMR (benzene-d_6) δ 161.48 (HC=*C*), 90.94 (*H*C=C), 53.64 (O*C*H$_3$), 49.61 (N*C*H$_3$), −9.58 (br, Al(*C*H$_3$)$_2$); M_w (cryoscopy, benzene) 332 (346). Recrystallization from diethyl ether at −30 °C afforded analytically pure **3b** as colorless crystals. Anal. Calcd for $C_7H_{16}NO_2Al$: C, 48.55; H, 9.31; N, 8.09. Found: C, 47.48; H, 8.54; N, 7.98.

$Et_2AlO(EtO)C{=}C(H)NEt_2$ (3c): yellow oil, isolated yield 97%; ^{1}H NMR (benzene-d_6) 4.08 (s, 1 H, *H*C=C), 3.75 (q, 2 H, OC*H*$_2$CH$_3$), 3.75 (q, 4 H, N(C*H*$_2$CH$_3$)$_2$), 0.00–1.60 (m, 19 H, OCH$_2$C*H*$_3$, N(CH$_2$C*H*$_3$)$_2$ and Al(C*H*$_2$C*H*$_3$)$_2$. Attempts to obtain solid samples of **3c** by crystallization were unsuccessful.

$Et_2AlO(t\text{-}BuO)C{=}C(H)NEt_2$ (3d): yellow oil, isolated yield 94%; ^{1}H NMR (benzene-d_6) 4.30 (s, 1 H, *H*C=C), 2.40 (q, 4 H, N(C*H*$_2$CH$_3$)$_2$), 1.39 (s, 9 H, OC(C*H*$_3$)$_3$), 1.30 (t, 6 H, Al(CH$_2$C*H*$_3$)$_2$), 0.68 (t, 6 H, N(CH$_2$C*H*$_3$)$_2$), 0.15 (q, 4 H, Al(C*H*$_2$CH$_3$). Attempts to obtain solid samples of **3d** by crystallization were unsuccessful.

$Me_2AlO(MeO)C{=}C(H)N(t\text{-}Bu)Me$ (3e): yellow oil, isolated yield 97%; ^{1}H NMR (benzene-d_6) δ 4.11 (s, 1 H, *H*C=C), 3.33 (s, 3 H, OC*H*$_3$), 2.12 (s, 3 H, NC*H*$_3$), 0.93 (s, 9 H, NC(C*H*$_3$)$_3$), −0.40 (s, 6 H, Al(C*H*$_3$)$_2$); ^{13}C NMR (benzene-d_6) δ 163.63 (HC=*C*), 84.03 (*H*C=C), 61.01 (N*C*(CH$_3$)$_3$), 53.23 (O*C*H$_3$), 42.06 (N*C*H$_3$), 25.14 (NC(*C*H$_3$)$_3$), −7.10 (br, Al(*C*H$_3$)$_2$). Attempts to obtain solid samples of **3e** by crystallization were unsuccessful.

General Procedure for the Synthesis of Dialkylaluminum Chloride Adducts (3′) of Dialkylaluminum Enolates 3. Adducts of **3′** can be obtained by addition of 2 equiv of dialkylaluminum chloride to preformed lithium enolates **2**, but compounds of a higher purity are obtained when pure dialkylaluminum enolates **3** are used as starting compounds. To a solution containing 10 mmol of a dialkylaluminum enolate **3** in 50 mL of benzene was added 10 mmol of a dialkylaluminum chloride (10.0 mL of a 1.0 M solution in hexanes) at room temperature. The resulting clear colorless solution was stirred for 1 h at room temperature, after which all volatile material was removed in vacuo affording the adduct **3′** with physical data as follows.

$Me_2AlO[(MeO)C{=}C(H)NMe_2]{\rightarrow}Al(Cl)Me_2$ (3b′): off-white solid, isolated yield 99%; ^{1}H NMR (benzene-d_6) δ 3.67 (s, 1 H, *H*C=C), 2.92 (s, 3 H, OC*H*$_3$), 1.61 (s, 6 H, N(C*H*$_3$)$_2$), −0.17 and −0.29 (s, 6 H, Al(C*H*$_3$)$_2$); ^{13}C NMR (benzene-d_6) δ 157.80 (HC=*C*), 92.08 (*H*C=C), 55.92 (O*C*H$_3$), 49.51 (N*C*H$_3$), −6.68 and −8.94 (br, Al(*C*H$_3$)$_2$). Recrystallization from diethyl ether at −30 °C afforded analytically pure **3b′** as colorless crystals. Anal. Calcd for $C_9H_{22}NO_2ClAl_2$: C, 40.69; H, 8.34; N, 5.27; Cl, 13.34. Found: C, 39.78; H, 7.98; N, 5.18; Cl, 14.09.

$Me_2AlO[(MeO)C{=}C(H)N(t\text{-}Bu)Me]{\rightarrow}Al(Cl)Me_2$ (3e′): pale yellow solid, isolated yield 97%; ^{1}H NMR (tol-d_8) δ 3.81 (s, 1 H, *H*C=C), 2.94 (s, 3 H, OC*H*$_3$), 1.88 (s, 3 H, NC*H*$_3$), 0.75 (s, 9 H, NC(C*H*$_3$)$_3$), −0.11 (s, 3 H, AlC*H*$_3$), −0.19 (s, 6 H, Al(C*H*$_3$)$_2$), −0.28 (s, 3 H, AlC*H*$_3$); ^{13}C NMR (tol-d_8) δ 158.40 (HC=*C*), 87.21 (*H*C=C), 61.85 (N*C*(CH$_3$)$_3$), 56.07 (O*C*H$_3$), 45.52 (N*C*H$_3$), 25.11 (NC(*C*H$_3$)$_3$), −3.97 (AlCH$_3$), −6.11 (Al(*C*H$_3$)$_2$), −7.11 (AlCH$_3$).

X-ray Data Collection, Structure Determination, and Refinement of $[Me_2AlO(MeO)C{=}C(H)NMe_2]_2$ (3b). A colorless crystal, obtained by crystallization from toluene at −80 °C, was sealed under nitrogen in a

Table V. Summary of X-ray Diffraction Data of **3b** and **3b′**

	Crystal Data	
formula	$C_{14}H_{32}N_2O_4Al_2$	$C_9H_{22}NO_2ClAl_2$
mol wt	346.38 (dimer)	265.69
space group	$P2_1/n$	$P2_1/n$
a, Å	8.095 (1)	9.456 (1)
b, Å	13.747 (1)	14.145 (1)
c, Å	9.641 (2)	12.208 (1)
β, deg	104.41 (1)	103.78 (1)
V, Å^3	1039.1 (3)	1585.9 (2)
Z	2	4
D_{calc}, g cm^{-3}	1.107	1.113
F(000), electrons	376	568
μ(Mo Kα), cm^{-1}	1.5	3.3
crystal dimen, mm	0.20 × 0.25 × 0.48	0.12 × 0.38 × 0.75
	Data Collection	
temp, K	295	295
radiatn, Å	0.71073	0.71073
2θ limits, deg	2.96–55.0	2.88–55.0
$\omega/2\theta$ scan, deg	0.60 + 0.35 tanθ	0.60 + 0.35 tanθ
ref refl	2-2-2, 2 3 0	0 2 0, 0 0 2, 4-3 0
no. of collected	5111	6894
obsd dat ($I > 2.5\sigma(I)$)	1138	2011
R(merge)	0.04	0.02
total X-ray exp time, h	58	41
decay, %	1	1.5
	Refinement	
R	0.056	0.051
R_w	0.057	0.043
w^{-1}	$\sigma^2(F) + 0.00049F^2$	$\sigma^2(F) + 0.000064F^2$
no. of refined parameters	121	163
S	0.71	0.73
final residual electron density, eÅ^{-3}	0.28	0.29

Table VI. Fractional Atomic Coordinates and Equivalent Isotropic Thermal Parameters (Å^2) with esd's in Parentheses for the Non-Hydrogen Atoms of **3b** and **3b'**

atom	x/a	y/b	z/c	U_{eq}
Al(1)	0.3787 (2)	0.42926 (8)	0.3930 (1)	0.0477 (4)
O(1)	0.4321 (3)	0.4679 (2)	0.5831 (3)	0.063 (1)
O(2)	0.3942 (3)	0.4681 (2)	0.8027 (3)	0.069 (1)
N(1)	0.1965 (4)	0.3354 (2)	0.4776 (3)	0.060 (1)
C(1)	0.3438 (5)	0.4303 (3)	0.6698 (3)	0.049 (1)
C(2)	0.3004 (5)	0.4383 (4)	0.9023 (4)	0.071 (2)
C(3)	0.2259 (5)	0.3645 (3)	0.6246 (4)	0.054 (2)
C(4)	0.2301 (9)	0.2304 (3)	0.4715 (7)	0.116 (3)
C(5)	0.0131 (6)	0.3522 (4)	0.4057 (5)	0.097 (2)
C(6)	0.5072 (6)	0.3242 (3)	0.3324 (6)	0.087 (2)
C(7)	0.2054 (6)	0.5044 (4)	0.2590 (5)	0.082 (2)
Al(1)	0.14930 (9)	0.39936 (7)	0.29652 (8)	0.0577 (3)
Al(2)	0.0789 (1)	0.18474 (7)	0.38975 (9)	0.0656 (4)
Cl(1)	0.30460 (9)	0.19735 (7)	0.3784 (1)	0.1077 (5)
O(1)	0.0297 (2)	0.3111 (1)	0.3445 (2)	0.0552 (7)
O(2)	−0.1858 (2)	0.2826 (1)	0.3785 (2)	0.0642 (8)
N(1)	−0.0275 (2)	0.4865 (2)	0.2681 (2)	0.0551 (9)
C(1)	−0.1045 (3)	0.3471 (2)	0.3415 (2)	0.048 (1)
C(2)	−0.3308 (3)	0.3092 (2)	0.3809 (3)	0.071 (1)
C(3)	−0.1377 (3)	0.4334 (2)	0.3066 (2)	0.054 (1)
C(4)	−0.0834 (4)	0.5093 (3)	0.1461 (3)	0.080 (1)
C(5)	0.0011 (4)	0.5774 (2)	0.3324 (3)	0.081 (2)
C(6)	0.2945 (4)	0.4493 (3)	0.4229 (3)	0.098 (2)
C(7)	0.1875 (5)	0.3672 (4)	0.1527 (3)	0.113 (2)
C(8)	−0.0278 (4)	0.1024 (3)	0.2728 (4)	0.111 (2)
C(9)	0.0738 (5)	0.1695 (3)	0.5474 (3)	0.116 (2)

Lindemann capillary and mounted on an Enraf-Nonius CAD-4F diffractometer. Crystal data and other numerical details of the structure determination are listed in Table V. Unit cell dimensions were calculated from the setting angles of 24 carefully centered reflections. The data of half of the reflection sphere ($+h, \pm k, \pm l$) were collected in the $\omega/2\theta$ scan mode, using Zr-filtered Mo Kα radiation, and corrected for Lorentz and polarization effects. The structure was solved by direct and difference-Fourier methods and refined on F by full-matrix least-squares techniques. Hydrogen atoms were introduced at calculated positions (C–H = 0.98 Å) and refined riding on their carrier atoms (except H on C(3), which was located in a difference Fourier map), with three common isotropic thermal parameters: one for the $Al(CH_3)_2$ and $N(CH_3)_2$ groups, one for the OCH_3 group, and one for HC=C, their final values amounting to 0.097 (9), 0.123 (6), and 0.07 (1) Å^2, respectively. The refinement converged at $R = 0.056$. Table VI lists the final positional parameters for the non-hydrogen atoms.

X-ray Data Collection, Structure Determination, and Refinement of $Me_2Al\overline{O[(MeO)C{=}C(H)NMe_2]}{\rightarrow}Al(Cl)Me_2$ (3b'). A pale yellow crystal, obtained by crystallization from toluene at −80 °C, was sealed under nitrogen in a Lindemann capillary and mounted on an Enraf-Nonius CAD-4F diffractometer. Crystal data and other numerical details of the structure determination are listed in Table V. Unit cell dimensions were calculated from the setting angles of 18 carefully centered reflections. The data of half of the reflection sphere ($\pm h, +k, \pm l$) were collected in the $\omega/2\theta$ xan mode, using Zr-filtered Mo Kα radiation and corrected for Lorentz and polarization effects. The structure was solved by standard Patterson and difference-Fourier methods and refined on F by full-matrix least-squares techniques. Hydrogen atoms were introduced at calculated positions (C–H = 0.98 Å) and refined riding on their carrier atoms (except H on C(3), which was located in a difference Fourier map) with five common isotropic thermal parameters: one for the $(CH_3)_2AlCl$, one for the $Al(CH_3)_2$, one for the $N(CH_3)_2$ groups, one for the OCH_3 group, and one for HC=C, their final values amounting to 0.171 (8), 0.153 (7), 0.101 (5), 0.089 (6), and 0.067 (9) Å^2, respectively. The refinement converged at $R = 0.051$. Table VI lists the final positional parameters for the non-hydrogen atoms. Scattering factors were taken from Cromer and Mann and corrected for anomalous dispersion.[22] The structure determination and refinement were carried out on an in-house micro-Vax minicomputer, with a locally adapted implementation of the SHELX-76 and SHELXS-86 packages.[23] All derived geometry calculations were performed with the programs of the EUCLID package.[24]

Acknowledgment. The research presented in this paper has been financially supported by Gist-brocades nv., The Netherlands and supported in part (A.L.S.) by the Netherlands Foundation for Chemical Research (S.O.N.) with financial aid of the Netherlands Organization for Advancement of Pure Research (N.W.O.). Dr. J. Boersma is kindly acknowledged for helpful discussions.

Supplementary Material Available: Tables of bond distances, angles, and anisotropic thermal parameters for non-hydrogen atoms and fractional coordinates and isotropic thermal parameters for hydrogen atoms (13 pages); tables with observed and calculated structure factors (38 pages). Ordering information is given on any current masthead page.

(22) (a) Cromer, D. T.; Mann, J. B. *Acta Crystallogr., Sect. A* **1968**, *A24*, 321. (b) Cromer, D. T.; Liberman, D. *J. Chem. Phys.* **1970**, *53*, 1891.
(23) (a) Sheldrick, G. M. SHELX-76. Program for Crystal Structure Determination; University of Cambridge: Cambridge, England. (b) Sheldrick, G. M. SHELXS-86. Program for Crystal Structure Determination; University of Göttingen: Göttingen, Federal Republic of Germany.
(24) Spek, A. L. In *Computational Crystallography*; Sayre, D., Ed.; Clarendon Press: Oxford; 1982; p 528.